Applied Catalysis B: Environmental 148–149 (2014) 424–435

Contents lists available at ScienceDirect

Applied Catalysis B: Environmental

journal homepage: www.elsevier.com/locate/apcatb

Functionalization of carbon xerogels for the preparation of palladium supported catalysts applied in sugar transformations

Nathalie Mager[a], Nathalie Meyer[a], Alexandre F. Léonard[b], Nathalie Job[b], Michel Devillers[a], Sophie Hermans[a,*]

[a] Université catholique de Louvain, Institut de la Matière Condensée et des Nanosciences (IMCN), Place Louis Pasteur 1, B-1348 Louvain-la-Neuve, Belgium
[b] Université de Liège, Laboratoire de Génie chimique-Génie catalytique, Institut de Chimie, bâtiment B6a, Sart-Tilman, B-4000 Liège, Belgium

ARTICLE INFO

Article history:
Received 6 August 2013
Received in revised form 31 October 2013
Accepted 17 November 2013
Available online 24 November 2013

Keywords:
Carbon xerogel
Functionalization
Lactose
Cellobiose
Bifunctional

ABSTRACT

Carbon xerogels with various pore textures were functionalized by HNO_3 or air to increase the number of acidic functions on their surface. These oxidized materials were systematically thermally treated to remove the unstable functions. Analyses indicated that the air treatment was the most efficient because the functions created are more numerous, more stable and homogeneously distributed within the support. These surface oxygenated groups were used as anchors for the covalent grafting of the complex $[Pd(OAc)_2(Et_2NH)_2]$ through a ligand exchange mechanism. Activation was carried out thermally to produce supported Pd nanoparticles and led to less sintering compared to a control catalyst prepared on an unmodified support. Catalysts were tested in two different catalytic reactions, namely lactose oxidation and hydrolytic oxidation of cellobiose. The former requires as few surface functions as possible while the latter demands a bifunctional catalyst for hydrolysis followed by oxidation. The oxidation of lactose was more efficient with the catalyst prepared on an unmodified carbon xerogel. On the opposite, the hydrolytic oxidation of cellobiose worked the best with a low loaded catalyst prepared on a functionalized support, which provided the acidic functions needed for hydrolysis. Moreover, 100% selectivity for gluconic acid was achieved.

1. Introduction

Carbonaceous materials are widely used as heterogeneous catalyst supports. Their advantages are numerous: they are inert, cheap, stable in aqueous media and mechanically robust. They are generally produced from organic matter like wood, coal or agro-food industry waste, display large specific surface areas and can be used under various forms [1–4]. The fact that their textural properties as well as the level of contaminant depend greatly on the origin of the raw material or of uncontrollable factors like weather conditions and soil composition is however a major drawback [4–6]. Therefore much research has been carried out in order to prepare synthetic carbonaceous materials, with control over textural properties, composition and surface chemistry. The first porous synthetic carbon materials were prepared by Pekala by polycondensation of resorcinol and aldehyde using a sol–gel method followed by drying and pyrolysis [7]. Unfortunately, drying by simple evaporation causes the material to shrink and crack, yielding then mostly non-porous carbon [8]. The gel was therefore dried under supercritical conditions. These materials were named "organic aerogels" [7,9]. Other drying methods were found to be effective, like solvent exchange followed by evaporation or freeze-drying, the latter leading to "cryogels" [10]. But since these methods remain difficult, expensive and time consuming, other synthetic routes were studied.

A more recent study has shown that evaporative drying of gels prepared under appropriate conditions and with controlled pH affords highly porous carbon materials with controllable pore texture. These are called "carbon xerogels" [11,12]. Like other carbonaceous materials, it is possible to increase the number of oxygenated groups at their surface to enhance the surface reactivity and hydrophilicity. This is done by an oxidation treatment in the gas or liquid phase and is called functionalization [13]. Liquid-phase functionalization involves stirring solid carbon in an oxidative solution, such as HNO_3, H_2O_2 or $(NH_4)_2S_2O_8$ [14–23,5]. HNO_3 is commonly used because its oxidative properties can be controlled with temperature, concentration and duration [24]. Although the harsh conditions associated with the HNO_3 solution may modify the textural properties of the material, it was found that it is minimized under mild conditions [25]. Gas-phase functionalization requires oxidation in a flow of air, O_2, O_3 or N_2O, for example [16,26,27].

* Corresponding author. Tel.: +32 10 472810; fax: +32 10 472330.
E-mail address: sophie.hermans@uclouvain.be (S. Hermans).

0926-3373/$ – see front matter © 2013 Elsevier B.V. All rights reserved.
http://dx.doi.org/10.1016/j.apcatb.2013.11.028

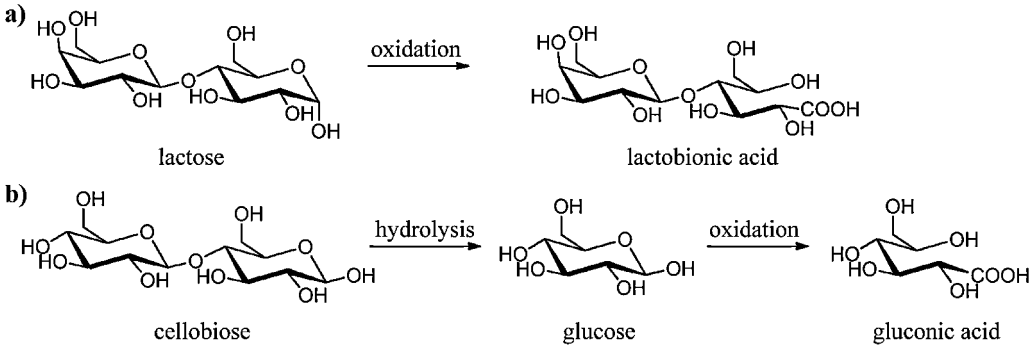

Fig. 1. Oxidation of lactose into lactobionic acid (a) and hydrolytic oxidation of cellobiose to gluconic acid (b).

It is commonly admitted that three main different oxygenated groups coexist on the surface of a carbonaceous material before or after functionalization, namely carboxylic acids, lactones and phenols, but there are also anhydrides and carbonyls [5]. Boehm and co-workers have developed a method to assess the number of these functions by titration, separately or altogether. Such a method also exists to estimate the number of basic functions [24]. The functionalization increases the amount of oxygen-containing groups while also improving the hydrophilicity of the support. This last point is significant when working in polar solvents like water during catalyst synthesis because it can also improve the interaction between the support and the precursor [3].

The preparation of noble metal catalysts on carbon modified by oxidation has been widely studied [28–30]. It is also known that oxygen surface groups can serve as anchors to graft metallic precursors [31–34]. During grafting, a chemical bond between the surface groups of a support and a metallic center is formed [35]. In theory, if the oxygenated functions are well dispersed, so will the metal particles arising from these grafted precursors [28].

Palladium-based catalysts have been very frequently investigated in the oxidation of sugars. Sugars represent one of the most important sources of renewable energy because they are independent from fossil fuels whilst being easily available, as some are considered as waste in the industry or because they are present in large quantities on earth. Moreover, they present a high chemical complexity [36–38]. At present time, most sugar transformations are carried out by fermentation or enzymatic processes [39]. Supported catalysts are less widely used because they tend to deactivate during sugar transformation. There is thus plenty of room for research in finding catalysts with high efficiency and long lifespan [40].

Many compounds can be produced from sugars with heterogeneous catalysts. Glucose can be transformed into gluconic acid, a chelating agent and food additive, with Bi–Pd/C catalysts [41,42]. Lactose, which is a disaccharide with a glucose subunit, can also be oxidized using Pd/BN (boron nitride), Pd/C or Pd/Al_2O_3 catalysts into lactobionic acid, which finds application in cosmetics or medicine [36,43,44]. The hydrolytic oxidation of cellobiose into gluconic acid as depicted in Fig. 1 is more challenging because it needs a bifunctional catalyst. The first step of hydrolysis is indeed to disconnect the β-1,4-glycosidic bond between the two D-glucose units, which requires acidic functions. The second step is oxidation, which needs metal particles with redox properties. Moreover, cellobiose can be viewed as a simple model of cellulose, which is an important non-edible source of biomass but whose selective conversion under mild conditions remains a challenge [37]. The catalytic conversion of this substrate could help providing efficient routes for the larger use of cellulose as raw material and has therefore been given much interest recently [45–50]. Up to now, the best catalyst is undoubtedly polyoxometalate supported gold, which gives both excellent yield and selectivity [47]. Regarding carbon-supported catalysts, which are also worth studying because they seem to be relatively inert toward the conversion of gluconic acid, unlike typical metal oxides like MgO or Al_2O_3, the best yield so far was of 80% with a 0.5 wt.% Au/CNT catalyst [45].

In this work, oxygen groups on the surface of carbon xerogels were used as anchors for grafting palladium precursors, to yield bifunctional catalysts with redox and acidic sites. Our strategy implied first to functionalize carbon xerogels of different porosities with liquid (HNO_3 solution) and/or gas (air) phase treatment. The carbon xerogels were then systematically stabilized, in order to remove all unstable functions. The best oxidation treatment was determined thanks to Boehm's titration and XPS measurements. Secondly, palladium precursors were grafted on these functions in a controlled manner and then activated thermally to cause reduction and coalescence into palladium nanoparticles. The stabilization treatment is important in order to avoid destruction of unstable functions too early during this activation step, and thus loss of dispersion of the metal particles. Indeed during the activation step the oxygenated function might decompose along with the complex and lead to a too high metal atoms mobility. Moreover, it is crucial to obtain stable acidic functions for the bifunctional catalysis. The formed catalysts were analyzed by XPS, TEM and dispersion measurements and the incidence of the oxidation treatments was studied. Finally some of the formed heterogeneous catalysts were tested in lactose oxidation (Fig. 1a) and for the two-steps hydrolytic oxidation of cellobiose into gluconic acid (Fig. 1b), where acidic functions are important for the hydrolysis step. The results were compared to allow a better understanding of the reactions needs in terms of catalytic materials.

The aim of the present study was to find an oxidation treatment able to introduce stable oxygenated functions at the surface of xerogels, that could be used to graft Pd complex precursors and as active site in a reaction requiring bifunctional catalysts.

This paper is organized as follows. First, the results of the functionalization of carbon xerogels are presented and discussed. Secondly, the experiments concerning the grafting and activation of palladium are reported and analyzed. Finally the catalytic results are depicted, which leads to conclusions.

2. Experimental

2.1. Materials

The carbon xerogels were synthesized according to the literature [11] and as described below. Aqueous organic gels were synthesized by polycondensation of 9.91 g of resorcinol [Vel, 99%] solubilized in 18.8 mL of water, with 13.5 mL of formaldehyde [Aldrich, 37% in water, stabilized with 10–15% methanol], in the presence of sodium hydroxide [Sigma, 97%] to adjust the pH, a

Table 1
Pore texture of the carbon xerogels.

Xerogel sample name	Synthesis pH	Type of solid	S_{BET} (m^2/g)	V_{DUB} (cm^3/g)	V_p (cm^3/g)	$V_{cum<7.5\ nm}$ (cm^3/g)	V_{Hg} (cm^3/g)	V_V (cm^3/g)	d_p (nm)
A	6.3	Micro–meso	671	0.27	0.60	–[b]	n. m.[d]	0.60[e]	10[f]
B	5.8	Micro–meso	772	0.29	1.10	–[b]	n. m.[d]	1.10[e]	27[f]
C	5.0	Micro–macro	598	0.24	–[a]	0.04	2.1	2.4	141[g]
D	4.0	Micro–macro	620	0.25	–[a]	<0.01[c]	2.0	2.2	400[g]
E	2.0	Micro–macro	604	0.24	–[a]	<0.01[c]	1.9	2.1	5500[g]

[a] Not pertinent due to the inaccuracy of the value (macroporous solids).
[b] Not calculated, the solid being micro-mesoporous.
[c] Below the error limit of the device.
[d] Not measured: since the solid is micro-mesoporous, nitrogen adsorption is sufficient to characterize the sample porosity.
[e] Equal to V_p (mesoporous solid).
[f] Micro-mesoporous sample: the average mesopore diameter is obtained from the nitrogen adsorption (Broekhoff-de Boer method).
[g] Micro-macroporous sample: the average macropore diameter is obtained from Hg porosimetry (Washburn's equation).

crucial variable in the control of textural properties (Table 1). After gelation, the samples were dried by evaporation under vacuum and pyrolyzed in order to obtain carbon samples of different porosities. The carbon xerogels were then ground and sieved to keep only the fraction of granulometry at 50–100 μm. These were submitted to oxidation treatment (i) in the liquid phase with HNO_3 [Acros, p.a.] of various concentrations (with 25 or 50 mL of solution for 1 or 2 g of carbon xerogel, respectively) at reflux (around 120 °C) for 24 h, then filtered out, washed on a Soxhlet apparatus for 24 h and dried under vacuum in an oven at 50 °C for 4 h, or (ii) in the gaseous phase in an oven at 350 °C for 3 h under an air flow of 0.4 dm^3/min with a heating rate of 10 °C/min [26]. The oxidized carbon xerogels were then stabilized in a tubular oven at 500 °C for 8 h under nitrogen flow with a temperature raise of 100 °C/h.

Carbon xerogel-supported palladium catalysts were prepared using carboxylate palladium complexes as precursors. The selected complex was synthesized as reported in the literature [51]: diacetatobis(diethylamine)palladium (II) $[Pd(OAc)_2(Et_2NH)_2]$ resulted from direct reaction of palladium acetate [Rocc, Pd 47.27%] with diethylamine [Sigma Aldrich, 98%] (yield: 76%). IR (KBr pellet): ν_{as}(COO) 1590, ν_s(COO) 1377 cm^{-1}. TGA: anal. (calcd.): 72.4% (71.3%). Elemental analysis: anal. (calcd.): C: 38.64 (38.87), H: 7.57 (7.61), N: 7.80 (7.56), Pd: 27.86 (28.70) %. The synthesized complex $[Pd(OAc)_2(Et_2NH)_2]$ was then grafted onto the various samples of treated carbon supports under the following conditions. The precursor was dissolved in distilled water and stirred with a fixed amount of carbon, in order to get 5 or 1 wt.% loading in the final catalysts, at room temperature for 24 h. The grafted materials were then filtered out, washed abundantly with water and dried under vacuum in an oven at 50 °C for 5 h or in the fume hood for 2–3 days in the case of the most powdery samples. The filtrates were kept for analysis by atomic absorption spectroscopy.

The grafted materials obtained were activated by heating in a tubular oven. They were heated to 200 °C under a flow of nitrogen with a heating rate of 100 °C/h, submitted for 1 h to a flow of hydrogen at 200 °C, and finally cooled down under nitrogen.

The different samples were designated as follows: the five prepared carbon xerogels were named A, B, C, D and E after their increasing average meso/macropore width, like listed in Table 1; functionalization treatment was specified using the words 'acid' or 'air' for the oxidizing treatment with nitric acid or air, respectively; concentration of nitric acid used in the liquid phase functionalization treatment was outlined by the numbers 2.5, 1.0 and 0.2 following the word 'acid' for a concentration of 2.5 mol/L, 1.0 mol/L and 0.2 mol/L, respectively; carbon xerogel that was not submitted to any functionalization treatment was named 'unmodified'; stabilization treatment was mentioned only if relevant by the word 'stabilized' (as all the supports used were systematically stabilized after functionalization and before grafting); palladium loading of the catalysts was specified by Pd5 and Pd1 for the initial Pd(5 wt.%) and Pd(1 wt.%) loaded samples, respectively. For example, Pd5/A-acid-1.0 designates the carbon xerogel of average mesopore width of 10 nm which was functionalized with a solution of nitric acid 1.0 mol/L and stabilized and with 5 wt.% loading of palladium.

2.2. Characterization methods

The Boehm's titration method developed by Boehm et al. and recently standardized [52,53], was used to assess the amount of some oxygen surface groups on the carbon materials, namely carboxylic acids, lactones and phenols, since carbonyl and ether groups cannot be quantified with this particular procedure. This method works on the principle that these oxygen groups have different acidities and can be neutralized by bases of different strengths. Experimentally, the surface groups are neutralized by an excess of the selected base, followed by back titration with hydrochloric acid. In this study, only sodium hydroxide was used as a base, which allows the neutralization (hence the quantification) of the sum of all phenol, lactone, and carboxylic acid groups, leading to a value named "total acidity" and expressed in mmol/100 g of carbon. In a typical experiment, 50 mL of NaOH 0.05 mol/L [FIXANAL, Riedel-de-Haën] is brought in contact with 0.40–0.50 g of carbon, and the mixture is stirred for 24 h at room temperature. The carbon is then filtered out, and the filtrate is titrated by fractions of 10 mL with hydrochloric acid, using phenolphthalein as an indicator. All these steps were carried out under nitrogen or argon flushing, using freshly distilled decarbonated water.

X-ray photoelectron spectroscopy (XPS) was carried out on a SSI-X-probe (SSX-100/206) Fisons spectrometer. The powder samples were pressed on small brass cups using double-face adhesive tape and then placed on an insulating homemade ceramic sample holder (Macor, Switzerland). A nickel grid was fixed 3 mm above the samples, and an electron flood gun was set at 8 eV to overcompensate for the positive charging of the samples during the analyses. The analyzed area was approximately 1.4 mm^2, and the pass energy was set at 150 eV. The binding energies were set by fixing the C1s peak [C—(C,H) component] at 284.8 eV. Three photopeaks (C1s, O1s and N1s) were systematically analyzed for the carbonaceous materials. The Pd3d peak was added for the catalysts. The XPS results were decomposed with the CasaXPS software using a sum of Gaussian/Lorentzian (85/15) after subtraction of a Shirley-type baseline. The constraints used for decomposition of the Pd3d peak were as follows: imposing an area ratio $Pd3d_{5/2}/Pd3d_{3/2}$ of 1.5, a difference in the binding energies ($Pd3d_{5/2}$–$Pd3d_{3/2}$) of 5.26 eV, and a FWHM ratio (for the $Pd3d_{5/2}/Pd3d_{3/2}$ peaks) of 1.

The pore texture of the carbonaceous materials was characterized by nitrogen adsorption–desorption as well as mercury intrusion porosimetry. The nitrogen adsorption–desorption isotherms were measured using a Micromeritics ASAP 2020 analyzer at −196 °C. Before analysis, the samples (0.02–0.10 g) were degassed for 10 h at 200 °C with a heating rate of 10 °C/min under 0.133 Pa pressure. The analysis of the isotherms provided specific surface

area calculated with the Brunauer–Emmett–Teller (BET) equation, S_{BET}, and the micropore volumes (V_{DUB}, volume of pores of width lower than 2 nm) determined with the Dubinin–Astakhov method, and the pore volume calculated from the adsorbed volume at saturation, V_P. The mesopore size distribution was calculated using the Broekhoff-de Boer theory.

In the case of samples containing macropores, the nitrogen adsorption technique is not appropriate for the determination of pore widths and pore volumes. For that reason, mercury porosimetry was performed on ThermoScientific Pascal 140 and 240 porosimeters in a pressure range from 0.01 to 200 MPa. Analysis of mercury intrusion data enabled to obtain the pore volume (V_{Hg}) as well as the pore size distribution corresponding to pores of width > 7.5 nm.

As already mentioned, both nitrogen adsorption and mercury porosimetry have limitations. Pore volume measurements by nitrogen adsorption are not accurate enough for samples containing macropores (pores of width larger than 50 nm, corresponding to relative pressures $p/p_0 > 0.98$ following the Kelvin equation) whereas mercury porosimetry is limited to pores larger than about 7.5 nm. In the case of samples containing macropores, the total pore volume V_v was thus deduced from a combination of these two techniques [54]:

$$V_v = V_{DUB} + V_{cum<7.5\,nm} + V_{Hg}$$

where V_{DUB} takes into account pores of width lower than 2 nm, V_{Hg} is the specific pore volume measured by mercury porosimetry, and $V_{cum<7.5nm}$ is the cumulative volume of pores of width between 2 and 7.5 nm determined from the mesopore size distribution by the Broekhoff-de Boer theory. For samples containing micropores and mesopores only and whose isotherm displays a plateau at saturation, the nitrogen adsorption technique is sufficient for determining the total void volume; consequently, V_v and V_p are equal.

One must note that carbon xerogels can be described as a stacking of microporous nodules delimiting meso- or macroporous voids, the size of which can be varied upon controlling the synthesis parameters [11]. As a result, the pore size distribution is always bimodal: the materials display micropores, located inside the nodules, and meso/macropores of controlled size corresponding to the voids between the nodules. The meso/macropore average width, d_p, was determined from the meso/macropore size distribution, calculated either from nitrogen adsorption (using the Broekhoff-de Boer theory) or from mercury porosimetry data (via Washburn's equation [55]).

Metallic dispersion measurements were conducted by CO chemisorption also with the Micromeritics ASAP 2020 apparatus. Before analysis, the sample (0.3–0.5 g) was degassed at 200 °C for 4 h with a heating rate of 1 °C/min under 13,300 Pa pressure. During analysis, it was first swept by a helium flow for 30 min at 100 °C with a heating rate of 10 °C/min then heated at 350 °C for 15 min with a temperature raise of 10 °C/min, before being reduced under hydrogen flow for 2 h at 350 °C. Hydrogen was finally evacuated for 2 h and the sample brought back to room temperature with a rate of 10 °C/min, at which point it was subjected to a sequence of CO pulses. The metal dispersion was calculated from the cumulative amount of adsorbed CO using the software provided with the apparatus. An adsorption stoichiometry Pd:CO of 1:1 was considered.

The IR spectra were recorded on a Bruker FTIR spectrometer (type EQUINOX 55) at a resolution of 4 cm^{-1}. KBr pellets containing 1 wt.% of the complexes were realized and the measurements conducted between 4000 and 400 cm^{-1}.

The synthesized complex was characterized for elemental content by the MEDAC Ltd. Company for microanalytical and metal analysis services in Egham (England). The Pd content of several catalysts was also determined by ICP-OES by Medac after acid digestion overnight (sample is first charred using hot sulphuric acid and then oxidized with perchloric acid to form the solution to analyze). Oxygen content (direct measure, not difference) was also determined by Medac on a Thermo FlashEA1112 elemental analyzer, after pyrolysis of the sample under catalytic conditions that produces oxygen bound as carbon monoxide.

Thermograms were recorded on a combined TGA–DSC analyzer of TA Instruments (type SDT 2960), under a 100 cm^3/min nitrogen flow at a heating rate of 10 °C/min, between 20 and 500 °C. The sample (approximately 5 mg) was placed in an alumina container (70 μL).

The quantification of Pd in solution of grafting filtrates and catalytic tests was performed by atomic absorption analysis, using a Perkin-Elmer 3110 spectrometer equipped with an air-acetylene flame atomizer. The calibration curve (from 0.5 to 10.0 mg/L Pd) was realized with standard solutions obtained by dilution of a commercial palladium [1 g/L, Fluka] solution.

Topographic SEM images were obtained using a FEG Digital Scanning Microscope (DMS 982 Gemini from Leo), equipped with an energy dispersive X-ray system (EDAX Phoenix equipped with a Leap detector). The powder samples were pressed onto conducting double-face adhesive tape fixed onto 5 mm aluminum specimen stubs from Agar Scientific.

TEM images were obtained with a LEO 922 Omega Energy Filter Transmission Electron Microscope at 200 kV. The samples were suspended in hexane under ultrasonic treatment, and then allowed to settle to discard the biggest particles. A drop of the supernatant was deposited on a holey carbon film supported on a copper grid, which was dried overnight under vacuum at room temperature, before introduction in the microscope.

XRD analyses were performed with a D5000 Siemens diffractometer equipped with a copper source ($\lambda_{K\alpha}$ = 154.18 pm). The samples were supported on quartz monocrystals. The crystalline phases detected were identified by reference to the JCPDS-ICDD database.

2.3. Catalytic tests

The oxidation of lactose into lactobionic acid was carried out in a 600 mL thermostated double-walled glass reactor. The pH of the lactose solution was measured continuously by a combined AgCl/Ag Beckman electrode. An automatic titration device Metrohm 842 Titrando was used to neutralize the acids formed over time with a 0.1 M KOH solution [Riedel-de-Haën, ≥85%] and keep the pH at a constant value. Constant stirring was ensured by a mechanical stirrer (Heidolph RZR 2051 electronic). Oxygen was introduced in the solution using a bent glass tube under constant flow and controlled by a flowmeter. Several parameters were set following a previous optimization [43]. Experimentally, 300 mL of milliQ water were added to the reactor containing 1.08 g of monohydrated lactose [Fluka] in order to obtain a concentration of 10 mmol/L. When the temperature was set to 40 °C, the stirring rate to 1000 rpm and the oxygen flow to 0.5 dm^3/min, the pH was brought to 9 with the KOH solution. The test started when 0.30 g of the catalyst was added. After 4 h of reaction with continuous pH control to keep it constant at pH = 9, the catalyst was recovered by filtration and the filtrate, brought to 1 L, was analyzed by HPLC.

HPLC analysis was performed on a Waters system equipped with a refractive index 2414 detector and a UV 2998 Photodiode Array detector. To quantify the lactose, a Transgenomics CARBOSep CHO-682 LEAD column was used, with milliQ water as eluent, a flow rate of 0.4 cm^3/min, a column temperature of 80 °C and 10 μL of injected volume. To quantify the lactobionic acid, an Aminex BioRad HPX-87 C column was used, with $CaSO_4$ [Dehydrated, ≥98%, Sigma Aldrich] 1.2 mmol/L solution as eluent, a

Table 2
Characterization of unmodified and functionalized supports, before and after stabilization.

Support and treatment	Unmodified XPS O/C (atomic)	Before stabilization		After stabilization	
		XPS O/C (atomic)	Total acidity (mmol/100g_C)	XPS O/C (atomic)	Total acidity (mmol/100g_C)
A-unmodified	0.06				
A-acid-0.2		0.14	135	0.07	32
A-acid-1.0		0.21	270	0.10	84
A-acid-2.5		0.20	245	0.10	64
A-air		0.19	276	0.11	133
B-unmodified	0.02				
B-acid-2.5		0.20	295	0.12	113
C-unmodified	0.04				
C-acid-1.0		0.14	182	0.08	70
C-air		0.14	243	0.09	124
D-unmodified	0.04				
D-air		0.14	232	0.10	98
E-unmodified	0.07				
E-air		0.18	274	0.13	137

flow rate of 0.8 cm^3/min, a column temperature of 80 °C and 10 μL of injected volume. The main by-product of lactose oxidation is 2-keto-lactobionic salt (overoxidation product) which is analyzed on the Aminex BioRad HPX-87 C column. The other potential by-products are lactulose (lactose's isomer), galactose and glucose (lactose's hydrolysis products) that could be analyzed on the CARBOSep CHO-682 LEAD column, but those were never spotted in the present study. Selectivity of the reaction was calculated using the equation: $\frac{\text{mmol lactobionic acid formed}}{\text{mmol lactose converted}} * 100$

The hydrolytic oxidation of cellobiose into gluconic acid was carried out in a 300 mL batch-type stainless steel autoclave from PARR. 0.77 g of cellobiose [Fluka, ≥99.0%] and 0.15 g of the catalyst were charged in the autoclave with 150 mL of milliQ water. A stirring rate of 1000 rpm was set before introducing oxygen in the reactor with a pressure of 500 kPa. Temperature was then set at 145 °C. When reaching this temperature, the test was continued for 3 h before being stopped by cessation of the stirring and cooling of the system to RT with cold water circulation in the outer mantel. The catalyst was then recovered by filtration and the filtrate, brought to 1 L, was analyzed by HPLC. No pH regulation was carried out during these tests.

HPLC analysis was performed on the same system as described above. Gluconic acid, the product of interest, as well as the potential overoxidation products (including for example acetic acid, glycolic acid, oxalic acid, succinic acid [47], acetylpropionic acid, glucuronic acid, glyceric acid or malic acid [46]) were quantified with the Aminex BioRad HPX-87C column, using the same conditions as above. Cellobiose and glucose, the reaction intermediate, were analyzed with the CARBOSep CHO-682 LEAD column. Because, in all cases, no by-products were observed, the quantification of the gluconic acid only was used for yield determination.

3. Results and discussion

3.1. Functionalization of carbon supports

Carbon xerogels of different porosities were prepared. The pore texture characterization data of the five supports are presented in Table 1 and the nitrogen isotherms in Fig. S1. Five xerogels of very different pore textures, ranging from micro-mesoporous to micro-macroporous, with meso/macropore sizes increasing from 10 to 5500 nm as the synthesis pH decreases, were obtained.

The functionalization of these supports was performed following two different methods. The first one takes place in the liquid phase, at reflux in a HNO_3 solution (of concentration 0.2, 1.0 or 2.5 mol/L). The second one occurs in the gaseous phase, in an oven under air. Not every support was submitted to both treatments. A slight degradation was observed, detected by the colored Soxhlet extraction waters, when the liquid phase functionalization was performed on larger average meso/macropore width samples. For this reason the supports D and E were submitted to air functionalization only. After functionalization, all the carbon xerogels were stabilized in a tubular oven at 500 °C under nitrogen flow to remove the unstable functions, mostly carboxylic groups. The supports were characterized by Boehm's titration and/or XPS in order to determine the degree of functionalization, before and after stabilization. It is important to keep in mind that XPS gives an estimation of the surface of the support only while the Boehm's titration can be considered as a bulk analysis, assessing the oxygenated functions of the whole accessible surface.

When both characterization methods were carried out on functionalized support before stabilization, a correlation between the total acidity measured by Boehm's titration and the O/C surface atomic ratios measured by XPS was found (Fig. S2(a) and (b)). Table 2 presents XPS results for the unmodified support as well as XPS and Boehm's titration results for the functionalized supports, before and after stabilization (more data for the unmodified supports is listed in Table S1). The O/C surface atomic ratios show that the unmodified carbon xerogels already contain some surface oxygenated groups. Any functionalization treatment increases them significantly. In the case of treatment with HNO_3 solution, the quantity of these groups is influenced by the acid concentration. However there seems to be a limit to this increase, as suggested by the fact that the A-acid-2.5 sample presents practically the same amount of surface oxygenated groups as the A-acid-1.0 sample. The amount of total acidic functions assessed by Boehm's titration is even lower for the A-acid-2.5 sample than for the A-acid-1.0. A slight degradation might occur under harsh conditions, as already observed with activated carbon [31]. In the case of treatment in the gaseous phase, the samples undergo a limited combustion. However the mass loss is not too important and reproducible for samples from the same batch (Table S2), except in one case (A).

After functionalization, all the samples underwent a stabilization treatment at 500 °C under nitrogen in order to remove the unstable functions. These functions are carboxylic acids and the existence of carboxyl groups on energetically different carbon sites or with different acid strengths has been admitted. Using TPD measurements, strongly acidic carboxylic groups were seen to form CO_2 around 260–330 °C while weakly acidic carboxylic groups formed CO_2 around 430–480 °C, in functionalized carbon xerogels

Table 3
Relative concentration of each component resulting from the decomposition of C_{1s} peak (XPS).

Support and treatment	I (%) C—C, C—H	II (%) C—O	III (%) C=O	IV (%) O—C=O	V (%) shake-up
A-unmodified	69.98	14.30	7.28	5.31	3.14
A-acid-2.5	65.60	15.72	10.15	5.73	2.81
A-acid-2.5 stabilized	71.24	14.95	6.72	4.69	2.39
A-air	65.79	17.49	9.07	5.50	2.14
A-air stabilized	68.10	15.79	7.46	5.40	3.27
B-unmodified	79.94	12.96	5.72	4.50	2.88
B-acid-2.5	65.21	14.90	10.63	6.16	3.11
B-acid-2.5 stabilized	66.95	15.50	8.22	5.83	3.50
C-unmodified	72.07	13.33	6.27	5.33	3.00
C-acid-1.0	67.95	14.79	8.92	5.36	2.98
C-acid-1.0 stabilized	70.61	15.38	6.77	5.06	2.17
C-air	64.26	18.93	7.81	5.23	3.37
C-air stabilized	67.96	15.77	7.48	5.78	3.01

[15,16,24,56,57]. Using complete Boehm's titration it was also proven that only half of the carboxylic acid functions were removed at 300 °C and that heating at 800 °C is needed to remove them completely, in activated carbon [58]. But at this temperature a lot of the other oxygenated functions are removed as well. Another study using complete Boehm's titration on activated carbon proved that the carboxylic acid functions were almost entirely removed and half of the phenols remained when a stabilization treatment at 500 °C was applied [59]. For these reasons, a 500 °C stabilization treatment was selected to obtain a solid with mainly phenols.

When the data before and after stabilization are compared in Table 2, it can be seen that the O/C surface atomic ratios drop strongly during stabilization but are still higher than those of the unmodified xerogels. Also, the atomic ratios are equal for the carbon xerogels A and C functionalized by both methods and under moderate conditions (HNO_3 1.0 mol/L). These XPS results were confirmed by the titration results, except for two differences: (i) the samples A-acid-1.0 and A-acid-2.5 have a noteworthy different total acidity while the O/C surface atomic ratios are the same; (ii) the samples A-air and C-air present a much higher total acidity than when treated in the liquid phase, whereas this difference is not that striking in the XPS results. Indeed the correlation between the total acidity and the O/C surface atomic ratios, presented in Fig. S3(a) and (b), is not as good as before stabilization. The explanation could be that there is a difference between the distribution of groups in the pores and at the external surface. Some functionalized and stabilized samples were ground and analyzed again by XPS (Fig. S4). All the samples functionalized under air displayed O/C surface atomic ratios quite unchanged after grinding. This indicates that the oxygenated groups were distributed homogeneously within the support. The A-acid-1.0 sample gave O/C surface atomic ratio doubled after grinding. This indicates that there were more oxygen functional groups inside the pores than at the external surface in the case of liquid phase functionalization. Elemental analysis (oxygen direct measure) done on the stabilized A-acid-1.0 and A-air samples indicates as well that A-acid-1.0 contains slightly more oxygen in mass than on the surface. The hypothesis to explain this unexpected result is that the acid stagnates inside the pores and more time is needed to remove it with the Soxhlet washing. Thereby the oxidation treatment would last longer inside the pores and create more oxygenated groups inside the pores than on the external surface.

Nitrogen adsorption measurements were carried out on two samples functionalized with the HNO_3 solution and under air in order to consider the general influence of each treatment on the texture (Fig. S5). The liquid phase treatment decreased the specific surface area, especially in the microporous area. This has already been mentioned in the literature when using concentrated nitric acid [20,58,60–62]. It is attributed to the creation of oxygenated groups at the entrance and/or the walls of micropores, resulting in pore blockage or by the possible destruction of the pore walls and their collapse when oxygenated terminal groups are created. On the contrary, the gas phase treatment increased the specific surface area, especially in the microporous area, as already mentioned also, due to relative pore enlargement by means of partial gasification of the carbon material [20,25].

It is possible to gain more qualitative information about the nature of the surface oxygenated groups using XPS [63]. The method is not accurate but is interesting when comparing similar supports. Given the differences met in the literature concerning the components found in each peak, a compromise was found [59]. The C_{1s} peak was deconvoluted into 5 component peaks with full width at half maximum constant for each component and equal to the main one. The main component peak was set at 284.8 eV and is due to graphitic carbon (C—C, C—H bonds, symbolized by **I** in Table 4). The other component peaks are attributed to carbon in alcohol or ether groups, assimilated to phenols (**II**), carbonyl groups, assimilated to lactones (**III**), carboxyl or ester groups (**IV**) and the 'shake-up electrons' (**V**). This decomposition of the C_{1s} peak is graphically presented in Fig. S6. It appears that the functionalization, whatever the treatment, increases the phenol, lactone and carboxylic acid functions (Table 3). Concerning the liquid phase treatment, the rise of the carboxylic functions is not as substantial as suggested before [14,16,58], because we used dilute solutions. However, one can see that the phenols increase a lot more with the air treatment than with HNO_3. After stabilization, all functions are partially removed for both treatments, but the phenols are still present in higher quantities with the air treatment. In all cases, after stabilization, the phenol and lactone functions are the main functions present on the surface of the supports. This explains why the total acidity of the A-air and C-air stabilized samples is much higher than their liquid phase counterparts, because this treatment adds a lot more phenol functions, that are less easily removed by stabilization.

The N_{1s} XPS zone was systematically analyzed for the functionalized and stabilized samples. It appears that the nitrogen surface concentration on the samples functionalized under air is negligible. This is not the case for the samples functionalized in the liquid phase, where the nitrogen surface concentration rises to around 1%. Furthermore bulk analysis of two A carbon xerogels functionalized by both methods (and stabilized) estimated the nitrogen concentration at around 0.76% for the sample treated in the HNO_3 solution while it was below the detection limit for the other one treated in air. This is attributed to nitro functions and to adsorbed nitrate ions resulting from the HNO_3 reactant [59,62–65].

To summarize, the treatment under air is more advantageous for the following reasons: it needs only 3 h instead of a bit more than 2 days when including the Soxhlet washings after liquid phase

oxidation; the formation of more stable oxygenated surface groups (phenols) is advantaged; the total acidity is higher after stabilization; the oxygen groups are homogeneously distributed within the porous support; and there is no contamination by nitrogen compounds. The good efficiency of the air treatment is explained by its faculty to be effective independently of the textural properties, as no diffusion problems arise, and not to be affected by the initial hydrophobicity of the carbon treated.

3.2. Grafting and activation

The oxygen functional groups introduced by functionalization on the carbon xerogels were used as anchors for the grafting of palladium precursors. These samples were afterwards activated in an oven under hydrogen at 200 °C to obtain palladium nanoparticles as active species.

3.2.1. Grafting of $[Pd(OAc)_2(Et_2NH)_2]$

The complex $[Pd(OAc)_2(Et_2NH)_2]$ was synthesized as described previously [51]. It was analyzed by TGA under nitrogen. All the ligands of the complex are removed at the temperature of 170 °C to yield metallic palladium as residue. Its choice as catalyst precursor was thus appropriate. From here, only the total acidity assessed by Boehm's titration will be taken into account when talking about the support acidity and not the XPS data. Indeed, the catalyst preparation experimental conditions are very similar to the titration conditions, by stirring the support in an aqueous solution for 24 h. This ensures that the accessible surface for the complex (during grafting) was the same as for the base (during titration).

The complex was used to prepare Pd(5 wt.%) and Pd(1 wt.%) catalysts on different functionalized and stabilized carbon xerogel samples. It was also introduced on an unmodified A sample which was used as control sample. Unlike the other samples, the unmodified A and the E-air xerogels presented a hydrophobic behavior: when added to the water solution, the carbon particles kept floating at its surface. While this appears logical for the unmodified support, the atomic O/C ratio cannot explain this behavior for the E-air xerogel. We think that this support is initially very hydrophobic and increasing the oxygenated surface groups like done here does not improve enough its hydrophilic properties. The synthesis filtrates were analyzed by atomic absorption to assess the amount of palladium incorporated within the samples. These results are expressed in experimental mass percentages of palladium in the sample and are presented in Table 4. Theoretical percentages are also presented, calculated on the basis of the amount of complex engaged in the syntheses. It can be seen that for most of the samples, a large amount, if not all, of the complex is indeed adsorbed, thanks to the known facile ligand exchange of carboxylate and diethylamine ligands for surface oxygen groups [31,51,59,66,67]. Significant differences between expected (calculated) and actual Pd loading are found to occur in only two cases, both with Pd(5 wt.%) catalysts: the A-unmodified sample, where the amount of adsorbed complex is lower than with the functionalized ones, and the E-air sample, where 69% of the palladium is not incorporated. It might be that the hydrophobic behavior of these two xerogel samples lessens the interaction between the support and the complex in aqueous solution. In the case of the E xerogel, this might also result from the difference of internal surface of this support compared to the others, micropores excluded. Actually, it is known that carbon xerogels are made of microporous nodules and display two types of pores: voids inside the nodules corresponding to micropores and voids between the nodules corresponding to meso- and macropores. Two surfaces may thus be considered: (i) the surface corresponding to micropores, located within the carbon nodules and (ii) the external surface of these nodules. Considering the size of the micropores, it is much probable that only the external surface of the nodules is available for the complex grafting. However, this surface decreases dramatically when the nodule size increases (i.e., when the pH decreases) and may be strongly limited for the support E in particular compared to the others [11]. It is possible to estimate the ratio between the surfaces of the nodules in two different samples. Since the amount of reagents is the same in all the samples, the volume of solid is nearly constant. If one considers that the nodules are spheres, one can demonstrate geometrically that the ratio between the surfaces of the nodules in two different samples, S_1/S_2, is equal to d_2/d_1, d_i being the average diameter of the nodules in the considered sample. From previous studies [11,12] one can estimate that the nodule diameter is *ca.* 10 nm in the case of sample A and *ca.* 5000 nm in the case of sample E. As a result, the external surface of the nodules is 500 times higher in the case of sample A, compared to sample E.

So, a large proportion of complex was incorporated on the Pd1/E-air sample however, probably because there are enough anchoring sites for the small Pd amount added. When comparing the two Pd5/A-air and Pd5/A-acid-1.0 samples, one can see that the amount of adsorbed complex is higher when it was functionalized under air, probably because of the higher total acidity (Table 2). Apart from that, no direct correlation between the total acidity of the support and the grafting efficiency was observed.

These grafted samples were analyzed by XPS. All functionalized xerogels show the presence of Pd^{II}, the binding energy of the $Pd3d_{5/2}$ peak being around 337.6 eV (Fig. S7 and Table S3). This makes sense as the oxidation state of the palladium precursor was +II and the adsorption mechanism is a ligand exchange and not a redox reaction. The ligand exchange occurs between a phenol function on the support and a carboxylate or a diethylamine ligand in the precursor complex (Fig. S8). Two close phenol functions can also operate, so the N/Pd surface atomic ratios (the N is corrected by subtracting the amount of N in each starting carbon) should be between 0 and 2 after grafting [31,59]. This was indeed the case for the samples prepared with the supports oxidized by air. However it does not fit when the supports were oxidized with HNO_3 because the large amount of nitro groups or nitrates obscures the diethylamine signal.

The Pd/C surface atomic ratios are depicted in Fig. 2. Concerning the Pd(5 wt.%) samples, Pd5/A-acid-1.0 has the highest Pd/C atomic ratio of 0.007 and Pd5/E-air the lowest, equal to 0.002. The other atomic ratios are comparable and stand around 0.005. In the case of Pd(1 wt.%) samples, Pd1/A-acid-1.0 has the largest Pd/C atomic ratio as well. No direct correlation between the total acidity of the supports and the Pd/C atomic ratio could be drawn either.

Table 4
Grafting of the complex $[Pd(OAc)_2(Et_2NH)_2]$ on the different samples of xerogels.

Initial loading	Support and treatment[a]	Mass percentage of palladium calculated[b]	Mass percentage of palladium found[c]
5 wt.%	A-unmodified	4.75	3.66
	A-acid-1.0	4.77	4.52
	A-air	4.76	4.75
	B-acid-2.5	4.78	4.49
	C-air	4.77	4.75
	D-air	4.76	4.70
	E-air	4.78	1.48
1 wt.%	A-acid-1.0	1.04	1.04
	A-air	0.99	0.99
	B-acid-2.5	0.99	0.99
	C-air	0.99	0.99
	D-air	0.99	0.99
	E-air	0.99	0.94

[a] All the functionalized supports were stabilized before grafting.
[b] Calculated on the basis of the amount of metallic precursor engaged in the synthesis
[c] Measured by analysis of the synthesis filtrate by atomic absorption

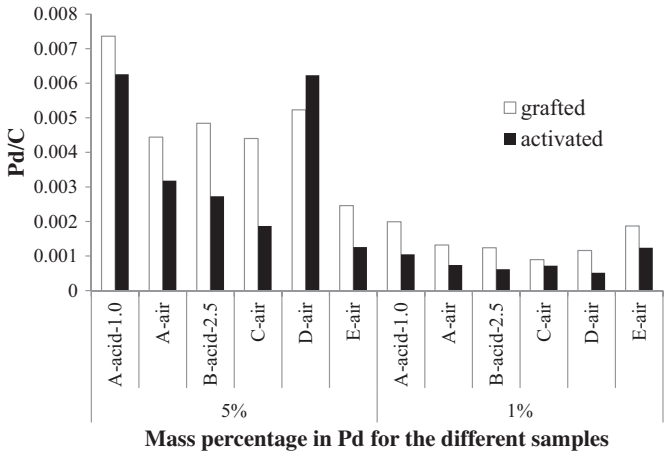

Fig. 2. Pd/C surface atomic ratios (XPS) for the grafted and activated samples.

The sample prepared with the unmodified support A is not depicted in Fig. 2 because of its too high Pd/C atomic ratio, equal to 0.051. XPS results also indicate that most of the metal present on the surface is in its reduced form (Fig. S7 and Table S3). In this case, the complex reduces itself at the external surface of the support because the oxygen functional groups are not numerous enough to stabilize it. The support being quite hydrophobic because of the few oxygenated surface groups, the palladium precursor does not enter much inside the pores and remains at the surface.

Some Pd5/xerogel-air were ground and analyzed again by XPS. The Pd/C atomic ratios remain unchanged, indicating a homogeneous distribution of the palladium within the sample. SEM (Fig. S9) and XRD (Fig. S10) analyses on the grafted samples did not show any agglomerate or crystalline particle, confirming that grafting actually occurred as expected to give molecular grafted species.

3.2.2. Activation of materials

Activation of the grafted samples was carried out in a tubular oven at 200 °C under hydrogen. First, the Pd loading of some samples after activation was checked by ICP-AES. The results were consistent with those obtained by atomic absorption analyses on synthetic filtrates shown in Table 4. In most cases, the XPS Pd/C atomic ratios decreased, dropping up to 50% of the initial atomic ratio, as shown in Fig. 2. This is due to coalescence of molecular grafted species into nanoparticles. Concerning the unmodified A sample, which had a Pd/C atomic ratio of 0.051 after grafting, its Pd/C atomic ratio dropped to 0.012 after activation. Sintering is thus more pronounced when the sample contains fewer oxygen groups to stabilize the grafted species, hence it is the worst for the unmodified support.

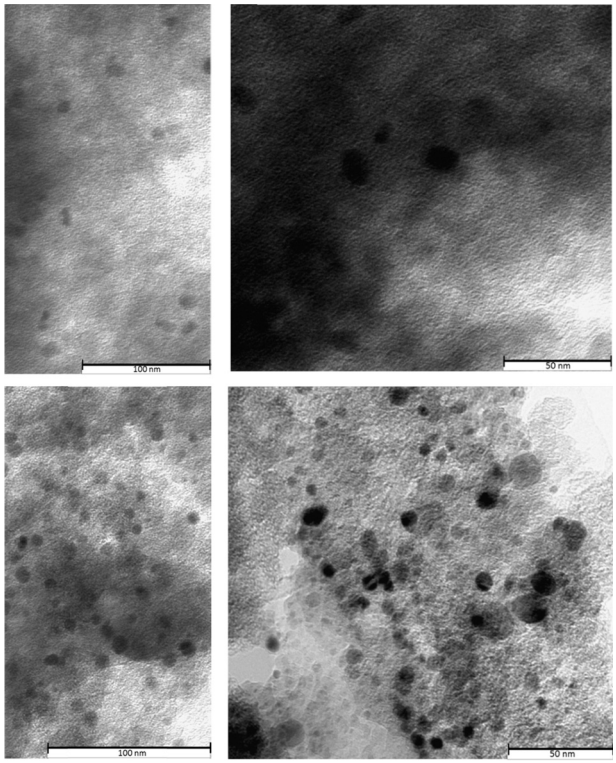

Fig. 3. TEM images of Pd1/A-acid-1.0 (above) and Pd1/A-air (beneath).

The activated samples present XPS $Pd3d_{5/2}$ peaks at 335.5 eV (Fig. S7 and Table S3), which corresponds to a shift of 2 eV compared to the grafted samples. This indicates that palladium is in its reduced form, as expected. Unfortunately, in the Pd(1 wt.%) samples, some oxidized palladium atoms seem to remain, maybe because low Pd loading caused anchoring through two surface groups, stabilizing the Pd^{II} oxidation state. However the peaks are not clearly distinguished from the background as seen in Fig. S11, due to the very low loading. Therefore it is difficult to undoubtedly assign each component.

TEM images of some samples allowed estimating the particle size after activation (Table 5 and Fig. S12). The two samples on carbon xerogel B display particles of the same size with a

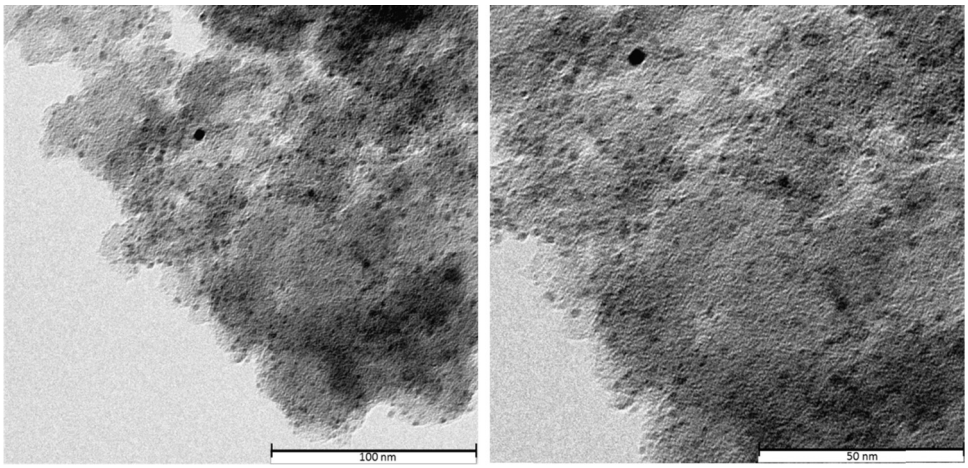

Fig. 4. TEM image of Pd5/A prepared on unmodified support.

Table 5
Pd dispersion measured by CO chemisorption and average particle size in nm estimated from TEM images.

Initial loading	Support and treatment	Pd mass percentage (%)	Average particle size (nm)	Pd dispersion (%)	Average particle size (nm)[a]
5 wt.%	A-unmodified	3.66	3	10.0	15.0
	A-acid-1.0	4.52	5–30	12.4	12.1
	A-air	4.75	/	10.3	14.6
	B-acid-2.5	4.49	5	8.7	17.2
	C-air	4.75	/	/[b]	/
	D-air	4.76	6	5.1	29.4
	E-air	4.78	50	6.9	21.7
1 wt.%	A-acid-1.0	1.04	14	0.4	374.6
	A-air	0.99	10	3.3	45.4
	B-acid-2.5	0.99	5	6.7	22.4
	C-air	0.99	/	/[b]	/
	D-air	0.99	/	3.7	40.5
	E-air	0.99	/	4.7	31.9

[a] Calculated from the dispersion measurements: $d_p = \frac{6 \text{ Molecular weight}}{\text{Dispersion} \times \text{Metal density} \times \text{Area occupied by each atom} \times \text{Avogardo number}}$.
[b] Undetermined due to sample powderness.

homogeneous distribution in both cases. No clear difference is observed, because the xerogel B has a large specific surface area which allows a good palladium distribution even at higher loading. When comparing all the samples prepared with the carbon xerogel A as support, it was first found that the sample Pd5/A-acid-1.0 yields a lot of agglomerates and a very wide particle size distribution. Secondly, the two samples Pd1/A provided us with a point of comparison between the two functionalization methods (Fig. 3). It appears that the sample functionalized under air presents particles of smaller size and better dispersion. Finally one can see that the unmodified support leads to the smallest and best dispersed particles (Fig. 4). Regarding the Pd5/E-air sample, the particle size is quite large and the metal not evenly distributed over the support. This is due to the hydrophobicity of the support or to the difference of internal surface, micropores excluded. Correlation between the average particle size and the dispersion measured by CO chemisorption was logically found. The Pd5/A-acid-1.0 stands out because of the broad particle size distribution: CO chemisorption gives an average value that is not related to TEM observations (Fig. S13). For the same reason, Pd5/E-air is not represented but stands out, probably because the particle size is not representative, as it is difficult to evaluate it by TEM due to the opacity of the sample (Fig. S12). Particle size was also calculated from the dispersion measurements, but one can see that these sizes are always higher than the measured ones, except for the Pd5/E-air whose measured size is not representative.

To summarize, the grafting of a palladium complex was successful when the support was functionalized and the loading did not depend on the textural properties of the carbon xerogel, except in one case. Functionalization under air guarantees an evenly dispersed complex inside the pores of the support. In the case of the unmodified support, grafting by ligand exchange does not occur as proven by the fact that most of the palladium is already in its reduced form before activation. Also, the loading is lower and the palladium mostly at the external surface when compared with functionalized xerogels, but the particles are smaller after activation (due to lower loading). During activation, coalescence occurs but is partially prevented by functionalization. The main differences regarding the location and the dispersion of the particles on the different supports are due to the textural and hydrophobicity properties of the xerogels. Finally, samples whose support was previously functionalized under air present particles of smaller and more homogeneous sizes than the supports functionalized in the liquid phase.

3.3. Catalytic tests

The catalytic performances of the synthesized catalysts were estimated in the two targeted reactions of sugar transformations. Most of the catalysts were tested in the oxidation of lactose into lactobionic acid while only a few of them were tested in the hydrolytic oxidation of cellobiose into gluconic acid, the latter requiring a bifunctional catalyst.

3.3.1. Oxidation of lactose

It has been reported that the metal–support interaction can have a negative influence on the catalytic activity [68]. More specifically, a previous work on Pd/BN catalysts has shown that the oxidation

Table 6
Catalytic performances of Pd catalysts for the oxidation of lactose.

Support and treatment	Pd mass percentage (%)	Lactobionic acid yield (%)	Lactobionic acid selectivity (%)[a]	TOF (s^{-1})[b]
A-acid	/	3	12	n.a.
Pd5/A-unmodified	3.66	30	100	0.0061
Pd5/A-acid-1.0	4.52	12	100	0.0014
Pd5/B-acid-2.5	4.49	26	92	0.0054
Pd5/C-air	4.75	4	100	/[c]
Pd5/D-air	4.76	16	100	0.0050
Pd5/E-air	4.78	1	12	0.0026
Pd1/A-acid-1.0	1.04	10	87	0.2052
Pd1/A-air	0.99	8	50	0.0342
Pd1/B-acid-2.5	0.99	2	100	0.0072
Pd1/C-air	0.99	6	87	/[c]
Pd1/D-air	0.99	1	8	0.0219
Pd1/E-air	0.99	3	28	0.0181

[a] Calculated from the lactose conversion and lactobionic acid yield.
[b] $\text{TOF} = \frac{\text{mol lactose converted}}{\text{mol Pd} \times \text{dispersion} \times \text{time}}$.
[c] Undetermined due to lack of dispersion data.

Table 7
Catalytic performances of Pd catalysts on support A for the hydrolytic oxidation of cellobiose.

Support and treatment	Pd mass percentage (%)	Gluconic acid yield (%)	Gluconic acid selectivity (%)	TOF (s^{-1})[a]
Pd5/A-unmodified	3.66	0	/	n.a.[c]
Pd5/A-air	4.75	15	100[b]	0.0045
Pd1/A-air	0.99	22	100[b]	0.0990

[a] $\text{TOF} = \frac{\text{mol lactose converted}}{\text{mol Pd} \times \text{dispersion} \times \text{time}}$.
[b] No peak of glucose or further oxidation products of gluconic acid were detected by HPLC.
[c] No cellobiose conversion was observed.

reaction of lactose is the most efficient and selective when the support contains no acidic groups [43,69]. To prove this point, catalytic tests were carried out with a wide range of catalysts, which differ in the loading, the support or the functionalization treatment of the support. The evolution of the activity with time is regular and all catalysts present parallel conversion curves (see Fig. S14 for 5 wt.% catalysts). There are no crossings during the first 4 h of the tests so comparisons between catalysts are allowed at t = 4 h. The yield and selectivity results are presented in Table 6, from which general trends can be extracted. First, one can see that the sample Pd5/B-acid-2.5 gives the best TOF value of the 5 wt.% loaded catalysts but that this support is the least active when comparing the 1 wt.% loaded catalysts. The catalysts on the support A and of 1 wt.% loading are the most active. The sample Pd1/A-acid-1.0 presents an abnormally high TOF, which can be explained by the very low dispersion. The catalysts made of the sample C have a lower yield than the catalysts on support A and furthermore, the sample powderness makes the analyses difficult to carry out. The catalysts on the supports D and E are quite active but give the worst results in terms of selectivity. Concerning the loading, one can see that the 1 wt.% loaded catalysts are the most active as seen by the TOF numbers but they present a less good selectivity. This is concordant with the previous observations with BN-supported catalysts as there are more acidic groups available and it has a negative effect in this reaction [43,69]. Moreover the catalyst prepared with the unmodified support is the best one for this reaction as shown by its highest TOF amongst the 5 wt.% loaded catalysts together with its excellent selectivity. This can be explained by the absence of surface acid functions and the homogeneous particle size distribution in this catalyst. When the samples Pd1/A-acid-1.0 and Pd1/A-air are compared, one can see that it is the catalyst with the support functionalized in the liquid phase that gives the best results, in selectivity as well as in yield, because as seen in Table 2 there are less oxygenated functions as determined by Boehm's titration. All these observations confirm the hypothesis that the oxidation of lactose into lactobionic acid needs a very inert support.

Moreover, some blank tests were run with (i) the support A-unmodified alone; (ii) the two A-acid-1.0 and A-air samples that underwent the same treatments as all the catalysts except for the palladium grafting. The supports unmodified and functionalized under air left the lactose intact. The support functionalized in the liquid phase however gave some lactobionic acid but with a very low selectivity (Table 6). This proves the need for palladium in this oxidation reaction and the negative influence of both the acidic functions and the probable NO_2 groups resulting from the functionalization treatment.

Correlation between the dispersion measured by CO chemisorption and the performance of the catalysts was found. It shows that the activity increases at lower dispersion (Fig. S15). This is in agreement with the literature where it was seen that too small particles have a negative influence in the oxidation of lactose [69].

In conclusion, we think that the support A is the best support for this reaction because at low loading these catalysts were the most effective and when the unmodified support was used it gave the smallest particles. Also, our observations indicate that there is no need for a functionalization treatment in this case since the support needed should contain the least possible oxygenated groups. In the future, a 1 wt.% loaded catalyst on an unmodified support could give better results than presented here. In this case, no grafting will occur and it will be interesting to proceed with in situ reduction to minimize the preparation time. Usual reducing agents, like $NaBH_4$ or formalin, or precipitation agents for a deposition-precipitation method, like NaOH, urea or Na_2CO_3, could be tested [43,69,70].

3.3.2. *Hydrolytic oxidation of cellobiose*

Only some selected catalysts were used in the hydrolytic oxidation of cellobiose with very different acidic properties in order to better understand the need for oxygenated functions in this second reaction. Catalysts prepared with the support A were selected because it was the most suitable for catalysis in the liquid phase as explained above. Results are shown in Table 7. The catalyst with the unmodified support does not produce any gluconic acid or glucose, which demonstrates the need for enough acidic functions on the support surface in order to hydrolyze cellobiose. Both catalysts prepared on functionalized supports are efficient for this two-step transformation. It can clearly be seen that the reaction is more efficient when the catalyst contains more remaining acidic functions available for catalysis i.e., with a lower Pd loading where less oxygen groups have been used up for grafting. Moreover these two catalysts are perfectly selective and no overoxidation occurs. Since no glucose is found in each case, the rate-limiting step seems to be the hydrolysis of cellobiose. Diminishing further the palladium loading should in this case give even better results.

One carbon-supported palladium catalyst was already reported for this reaction, namely a 0.5 wt.% Pd/CNT catalyst, but gave only a poor yield of 2.9%. Carbon xerogels, which were to the best of our knowledge used here for the first time in this reaction, seem more efficient and selective than CNT. The gold/CNT counterpart however gave an excellent yield, of 80% [45]. Another catalyst, 4 wt.% Pt/AC-SO_3H, presented a 46% yield for the same reaction [49]. The two latter results are better than what is presented here, even if byproducts are formed, certainly because these metals are better for the oxidation of glucose in general. Using these metals on carbon xerogel should thus improve our yields. Optimization of the reaction conditions would also be interesting to raise the yield.

Finally the catalysts found in the literature need at some point of their synthesis an oxidizing treatment in strong acidic solution like H_2SO_4 or HNO_3. The use of air as oxidizing agent for the carbonaceous support is a cleaner and more viable alternative that could also be used for cheaper materials like activated carbon. Moreover, the nature of the oxygen functional groups introduced (hydroxyls rather than carboxylic acids) is also advantageous because they are more stable.

4. Conclusion

It was found that the surface oxygenated groups on a carbon xerogel material could have a crucial double role, first in the

controlled preparation of Pd/C catalysts by grafting and secondly in bifunctional catalysis using their hydrolysis abilities.

Surface functionalization of xerogels was achieved using HNO_3 or air followed by stabilization and quantified by Boehm's titration and XPS analyses. The gaseous phase functionalization outperforms the liquid phase one because it is time-saving (it is a single step reaction), more efficient whilst creating more stable functions that are less removed during stabilization, namely phenols, more homogeneous and a lot cleaner (it does not use a strong acid). Moreover, the hydrophobic properties of some samples can affect the success of the functionalization in an aqueous solution while it is not the case for the air treatment, which explains its good performance.

Pd/C catalysts on different carbon xerogel supports previously functionalized and stabilized were prepared using the oxygen groups as anchors for covalent grafting of Pd complex precursors. An unmodified support led to mostly reduced palladium on the external surface before activation. After activation, this catalyst had the smallest particles. As there are practically no acidic functions on this support, the complex self-reduced directly and gave extremely small particles at the external surface that remained small even if sintering was important during activation. The grafting of $[Pd(OAc)_2(Et_2NH)_2]$ on functionalized supports occurred by a ligand exchange mechanism keeping Pd in its +II oxidation state and its relative success did not depend on the textural properties of the supports, except in one case. Activation reduced all the Pd^{II} into Pd^0 with some sintering, but less than on unmodified xerogel. Particles were more dispersed and of smaller size on air-functionalized supports than the liquid phase ones.

The catalyst prepared on unmodified support was very efficient in the reaction of lactose oxidation, this reaction needing the least possible surface functions. However it was not active at all in the hydrolytic oxidation of cellobiose into gluconic acid, the latter reaction needing acidic functions for the hydrolysis step. By opposition, the catalysts prepared on functionalized supports were able to perform bifunctional catalysis in a two-step reaction but were less active in the oxidation of lactose. The catalyst with the lower palladium loading gave a fair yield of gluconic acid from cellobiose and 100% selectivity. This study opens the door to further applications of bifunctional catalysts prepared by modification of the support to more challenging raw substrates.

Acknowledgements

The authors wish to thank the Fonds de la Recherche Scientifique (F.R.S.-FNRS) with the assistance of the Fédération Wallonie-Bruxelles and the Belgian National Lottery, as well as the Université catholique de Louvain for funding. This work was also partially funded by the Belgian State (Belgian Science Policy, IAP Project INANOMAT N° P6/17). We are grateful as well to Jean-François Statsijns for technical assistance.

Appendix A. Supplementary data

Supplementary data associated with this article can be found, in the online version, at http://dx.doi.org/10.1016/j.apcatb.2013.11.028.

References

[1] M.L. Toebes, J.V. van Dillen, K.P. de Jong, J. Mol. Catal. A: Chem. 173 (2001) 75–98.
[2] X. Hao, S. Barnes, J.R. Regalbuto, J. Catal. 279 (2011) 48–65.
[3] F. Rodríguez-Reinoso, Carbon 36 (1998) 159–175.
[4] E. Auer, A. Freund, J. Pietsch, T. Tacke, Appl. Catal. A: Gen. 173 (1998) 259–271.
[5] A. Polania, E. Papirer, J.B. Donnet, G. Dagois, Carbon 31 (1993) 473–479.
[6] C. Moreno-Castilla, J. Rivera-Utrilla, MRS Bull. 26 (2001) 890–894.
[7] R.W. Pekala, F.M. Kong, Rev. Phys. Appl. 24 (1989) 33–40.
[8] C. Lin, J.A. Ritter, Carbon 38 (2000) 849–861.
[9] R.W. Pekala, D.W. Shaefer, Macromolecules 26 (1993) 5487–5493.
[10] B. Mathieu, S. Blacher, R. Pirard, P.-P. Pirard, B. Sahouli, F. Brouers, J. Non-Cryst. Solids 212 (1997) 250–261.
[11] N. Job, R. Pirard, J. Marien, J.-P. Pirard, Carbon 42 (2004) 619–628.
[12] N. Job, A. Théry, R. Pirard, J. Marien, L. Kocon, J.-N. Rouzaud, F. Béguin, J.-P. Pirard, Carbon 43 (2005) 2481–2494.
[13] T.J. Bandosz, in: P. Serp, J.L. Figueiredo (Eds.), Surface Chemistry of Carbon Materials in Carbon Materials for Catalysis, Wiley, New Jersey, 2009, pp. 45–92.
[14] M. Santiago, F. Stüber, A. Fortuny, A. Fabregat, J. Font, Carbon 43 (2005) 2134–2145.
[15] A.M.T. Silva, B.F. Machado, J.L. Figueiredo, J.L. Faria, Carbon 47 (2009) 1670–1679.
[16] N. Mahata, M.F.R. Pereira, F. Suárez-García, A. Martínez-Alonso, J.M.D. Tascón, J.L. Figueiredo, J. Colloid Interface Sci. 324 (2008) 150–155.
[17] C. Moreno-Castilla, M.V. López-Ramón, F. Carrasco-Marín, Carbon 38 (2000) 1995–2001.
[18] C. Moreno-Castilla, F. Carrasco-Marín, A. Meuden, Carbon 35 (1997) 1619–1626.
[19] C. Moreno-Castilla, M.A. Ferro-Garcia, J.P. Joly, I. Bautista-Toledo, F. Carrasco-Marin, J. Rivera-Utrilla, Langmuir 11 (1995) 4386–4392.
[20] C. Alegre, M.E. Gálvez, E. Baquedano, E. Pastor, R. Moliner, M.J. Lázaro, Int. J. Hydrogen Energy 37 (2012) 7180–7191.
[21] J.S. Noh, J.A. Schwarz, Carbon 28 (1990) 675–682.
[22] P. Vinke, M. van der Eijk, M. Verbree, A.F. Voskamp, H. van Bekkum, Carbon 32 (1994) 675–686.
[23] C. Moreno-Castilla, F. Carrasco-Marín, F.J. Maldonado-Hódar, J. Rivera-Utrilla, Carbon 36 (1998) 145–151.
[24] H.P. Boehm, Carbon 40 (2002) 145–149.
[25] M.A. Fraga, E. Jordao, M.J. Mendez, M.M.A. Freitas, J.L. Faria, J.L. Figueiredo, J. Catal. 209 (2002) 355–364.
[26] C.C. Gheorghiu, M. Pérez-Cadenas, M.C. Román-Martínez, C. Salinas-Martínez de Lecea, N. Job, Stud. Surf. Sci. Catal. 175 (2010) 647–651.
[27] P.V. Samant, F. Gonçalves, M.M.A. Freitas, M.F.R. Pereira, J.L. Figueiredo, Carbon 42 (2004) 1321–1325.
[28] D.J. Suh, T.J. Park, Carbon 31 (1993) 427–435.
[29] F. Rodríguez-Reinoso, I. Rodríguez-Ramos, C. Moreno-Castilla, A. Guerrero-Ruiz, J.D. López-González, J. Catal. 99 (1986) 171–183.
[30] A. Guerrero-Ruiz, I. Rodríguez-Ramos, F. Rodríguez-Reinoso, C. Moreno-Castilla, D. López-González, Carbon 26 (1988) 417–423.
[31] S. Hermans, C. Diverchy, O. Demoulin, V. Dubois, E.M. Gaigneaux, M. Devillers, J. Catal. 243 (2006) 239–251.
[32] H.E. Van Dam, H. van Bekkum, J. Catal. 131 (1991) 335–349.
[33] C. Prado-Burguete, A. Linares-Solano, F. Rodríguez-Reinoso, C. Salinas-Martínez de Lecea, J. Catal. 115 (1989) 98–106.
[34] Y.A. Ryndin, O.S. Alekseev, P.A. Simonoc, V.A. Likholobov, J. Mol. Catal. 55 (1989) 109.
[35] F. Averseng, M. Vennat, M. Che, Grafting and anchoring of transition metal complexes to inorganic oxides, in: H. Drozinger, G. Ertl, F. Schüth, J. Weitkamp (Eds.), Handbook of Heterogeneous Catalysis, Wiley, Weinheim, 2008, pp. 522–539.
[36] J. Kuusisto, A.V. Tokarev, E.V. Murzina, M.U. Roslund, J.-P. Mikkola, D.Y. Murzin, T. Salmi, Catal. Today 121 (2007) 92–99.
[37] J.A. Geboers, S. Van de Vyver, R. Ooms, B. Op de Beek, P.A. Jacobs, B.F. Sels, Catal. Sci. Technol. 1 (2011) 714–726.
[38] M.L. Imhoff, L. Bounoua, T. Ricketts, C. Loucks, R. Harris, W.T. Lawrence, Nature 429 (2004) 870–873.
[39] D. Cannella, C.-W. Hsieh, C. Felby, H. Jørgensen, Biotechnol. Biofuels 5 (2012) 26.
[40] M. Besson, P. Gallezot, Catal. Today 57 (2000) 127–141.
[41] S. Ramachandran, P. Fontanille, A. Pandey, C. Larroche, Food Technol. Biotechnol. 44 (2006) 185–195.
[42] M. Wenkin, P. Ruiz, B. Delmon, M. Devillers, J. Mol. Catal. A: Chem. 180 (2002) 141–159.
[43] N. Meyer, K. Bekaert, D. Pirson, M. Devillers, S. Hermans, Catal. Commun. 29 (2012) 170–174.
[44] A.V. Tokarev, D.Y. Murzin, J. Mol. Catal. A: Chem. 255 (2006) 199–208.
[45] X. Tan, W. Deng, M. Liu, Q. Zhang, Y. Wang, Chem. Commun. (2009) 7179–7181.
[46] D. An, A. Ye, W. Deng, Q. Zhang, Y. Wang, Chem. Eur. J. 18 (2012) 2938–2947.
[47] W. Deng, Y. Wang, Q. Zhang, Y. Wang, Catal. Surv. Asia 16 (2012) 91–105.
[48] A. Onda, J. Jpn. Pet. Inst. 55 (2012) 73–86.
[49] A. Onda, T. Ochi, K. Yanagisawa, Catal. Commun. 12 (2011) 421–425.
[50] J. Zhang, X. Liu, M.N. Hedhili, Y. Zhu, Y. Han, ChemCatChem 3 (2011) 1294–1298.
[51] T.A. Stephenson, S.M. Morehouse, A.R. Powell, J.P. Herffer, G. Wilkinson, J. Chem. Soc. (1965) 3632–3640.
[52] S.L. Goertzen, K.D. Thériault, A.M. Oickle, A.C. Tarasuk, H.A. Andreas, Carbon 48 (2010) 1252–1261.
[53] A.M. Oickle, S.L. Goertzen, K.R. Hopper, Y.O. Abdalla, H.A. Andreas, Carbon 48 (2010) 3313–3322.
[54] C. Alié, R. Pirard, A.J. Lecloux, J.-P. Pirard, J. Non-Cryst. Solids 246 (1999) 216–228.
[55] E.W. Washburn, Proc. Natl. Acad. Sci. 7 (1921) 115–116.
[56] J.L. Figueiredo, M.F.R. Pereira, M.M.A. Freitas, J.J.M. Órfão, Carbon 37 (1999) 1379–1389.
[57] J.L. Figueiredo, M.F.R. Pereira, J. Energy Chem. 22 (2013) 195–201.
[58] Y.F. Jia, K.M. Thomas, Langmuir 16 (2000) 1114–1122.

[59] S. Hermans, C. Diverchy, V. Dubois, M. Devillers, Appl. Catal. A: Gen. (2013), http://dx.doi.org/10.1016/j.apcata.2013.09.029, in press.
[60] M. Carmo, M. Linardi, J.G.R. Poço, Appl. Catal. A: Gen. 355 (2009) 132–138.
[61] J. Jaramillo, P.M. Álvarez, V. Gómez-Serrano, Fuel Process. Technol. 91 (2010) 1768–1775.
[62] B.K. Pradhan, N.K. Sandle, Carbon 37 (1999) 1323–1332.
[63] L. Calvo, M.A. Gilarranz, J.A. Casas, A.F. Mohedano, J.J. Rodriguez, Ind. Eng. Chem. Res. 44 (2005) 6661–6667.
[64] H. Teng, E.M. Suuberg, J. Phys. Chem. 97 (1993) 478–483.
[65] P.A. Bazula, A.-H. Lu, J.-J. Nitz, F. Schüth, Microporous Mesoporous Mater. 108 (2008) 266–275.
[66] B. Milani, L. Vicentini, A. Sommazzi, F. Garbassi, E. Chiarparin, E. Zangrando, G. Mestroni, J. Chem. Soc. Dalton Trans. (1996) 3139–3144.
[67] N. Thirupathi, D. Amoroso, A. Bell, J.D. Protasiewicz, Organometallics 26 (2007) 3157–3166.
[68] G. Postole, M. Caldararu, N.I. Ionescu, B. Bonnetot, A. Auroux, C. Guimon, Thermochim. Acta 434 (2005) 150–157.
[69] N. Meyer, D. Pirson, M. Devillers, S. Hermans, Appl. Catal. A: Gen 467 (2013) 463–473.
[70] P. Mäki-Arvela, D.Y. Murzin, Appl. Catal. A: Gen. 451 (2013) 251–281.